Theoretical study of Λ resonances from an analysis of Crystal Ball $K^- p \to \pi^0\Sigma^0$ reaction data with center-of-mass energies of 1536–1676 MeV

Jun Shi[1] and Bing-Song Zou[1,2]

[1]*Institute of High Energy Physics and Theoretical Physics Center for Science Facilities, Chinese Academy of Sciences, Beijing 100049, China*

[2]*State Key Laboratory of Theoretical Physics, Kavli Institute for Theoretical Physics China, Institute of Theoretical Physics, Chinese Academy of Sciences, Beijing 100190, China*

(Received 4 November 2014; revised manuscript received 21 January 2015; published 3 March 2015)

With an effective Lagrangian approach, we analyze the $K^- p \to \pi^0\Sigma^0$ reaction to study the Λ hyperon resonances by fitting the Crystal Ball data on differential cross sections and Σ^0 polarization with the center-of-mass energies of 1536–1676 MeV. Besides well-established Particle Data Group (PDG) four-star Λ resonances around this energy range, the $\Lambda(1600)\frac{1}{2}^+$ resonance, listed as a three-star resonance in the PDG data, is found to be definitely needed. In addition, there is strong evidence for the existence of a new $\Lambda(\frac{3}{2}^+)$ resonance around 1680 MeV.

DOI: 10.1103/PhysRevC.91.035202 PACS number(s): 14.20.Gk, 13.75.−n, 25.75.Dw

I. INTRODUCTION

The $\overline{K}N$ scattering interaction has been widely used to study the hyperon resonances. In our previous work [1,2], we have analyzed the $K^- N \to \pi\Lambda$ reaction to study the Σ resonances; now we move forward to study the pure isospin-0 reaction $K^- p \to \pi^0\Sigma^0$ to identify the structures of the Λ resonances.

Many studies have been carried out to investigate the Λ resonances. Jido *et al.* [3] and Magas *et al.* [4] used a chiral unitary approach for the meson-baryon interactions and got two $J^P = \frac{1}{2}^-$ resonances with one mass near 1390 MeV and the other around 1420 MeV. They believe the well-established $\Lambda(1405)\frac{1}{2}^-$ resonance listed in the Particle Data Group (PDG) data [5] is actually a superposition of these two $\frac{1}{2}^-$ resonances. Zhang *et al.* [6] and Kamano *et al.* [7] conducted a multichannel partial-wave analysis of $\overline{K}N$ reactions and got results with some significant differences. Zhong and Zhao [8] analyzed the $K^- p \to \pi^0\Sigma^0$ reaction with the chiral-quark model and discussed characteristics of the well-established Λ resonances. Liu and Xie [9] analyzed the $K^- p \to \eta\Lambda$ reaction with an effective Lagrangian approach and implied a D03 resonance with a mass of about 1670 MeV but a much smaller width compared with the well-established $\Lambda(1690)\frac{3}{2}^-$. So there are still some ambiguities of the Λ resonant structures needing to be clarified.

Recently, the most precise data on the differential cross sections for the $K^- p \to \pi^0\Sigma^0$ reaction have been provided by the Crystal Ball experiment at the BNL Alternating Gradient Synchrotron [10,11]. The Σ^0 polarization data were presented for the first time. However, with different data selection cuts and reconstructions, two groups in the same collaboration, i.e., the VA group [10] and the UCLA group [11], got inconsistent results for the Σ^0 polarizations. Previous multichannel analysis [6–8] of the $\overline{K}N$ reactions failed to reproduce either set of the polarization data.

In the present work, instead of performing some sophisticated multichannel analysis, as the first step, we concentrate on the most precise data by the Crystal Ball (CB) Collaboration on the pure isospin scalar channel of the $\overline{K}N$ reaction to see what are the Λ resonances the data demand and how the two groups' distinct polarization data [10,11] influence the spectroscopy of Λ resonances. Consistent differential cross sections of earlier work by Armenteros *et al.* [12] at lower energies are also used.

This work is organized as follows. In Sec. II we present our theoretical evaluating procedure of the analysis. In Sec. III we show our study results and give relevant discussions. Finally, a brief summary is given in Sec. IV.

II. THEORETICAL FORMALISM

For the reaction $K^- p \to \pi^0\Sigma^0$, the basic contributions come from the t-channel K^* exchange, the u-channel proton exchange, the and s-channel Λ and its resonances. The corresponding Feynman diagrams are shown in Fig. 1. In addition to the t-channel and u-channel contributions, the s-channel contributions from five well-established four-star Λ and their resonances listed in the PDG data [5], $\Lambda(1115)\frac{1}{2}^+$, $\Lambda(1405)\frac{1}{2}^-$, $\Lambda(1520)\frac{3}{2}^-$, $\Lambda(1670)\frac{1}{2}^-$, and $\Lambda(1690)\frac{3}{2}^-$, are always included in our analysis.

In the t-channel K^* exchange process, the effective Lagrangians are

$$\mathcal{L}_{K^*K\pi} = i g_{K^*K\pi} K^*_\mu (\pi\cdot\tau\partial^\mu K - \partial^\mu\pi\cdot\tau K), \quad (1)$$

$$\mathcal{L}_{K^*N\Sigma} = -g_{K^*N\Sigma}\overline{\Sigma}\left(\gamma_\mu K^{*\mu} - \frac{\kappa_{K^*N\Sigma}}{2M_N}\sigma_{\mu\nu}\partial^\nu K^{*\mu}\right)N. \quad (2)$$

The $K^*K\pi$ coupling constant can be calculated from the decay width of $K^* \to K\pi$, getting $g_{K^*K\pi} = -3.23$, where the minus sign of the coupling is from SU(3) relations and relevant meson scattering phase shift data [13]. As for the $K^*N\Sigma$ couplings, Refs. [14,15] give two sets of values:

$$g_{K^*N\Sigma} = -2.46, \quad \kappa_{K^*N\Sigma} = -0.47(NSC97a),$$
$$g_{K^*N\Sigma} = -3.52, \quad \kappa_{K^*N\Sigma} = -1.14(NSC97f).$$

Thus we limit $g_{K^*N\Sigma}$ to be between −3.52 and −2.46, and $\kappa_{K^*N\Sigma}$ to be between −1.14 and −0.47.

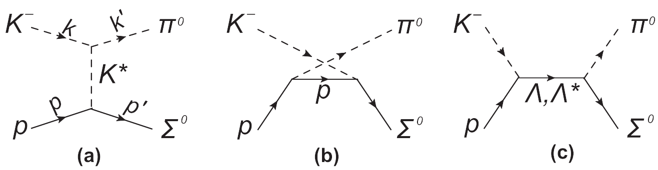

FIG. 1. Feynman diagrams for $K^- p \to \pi^0\Sigma^0$: (a) t-channel K^* exchange, (b) u-channel proton exchange, and (c) s-channel Λ and its resonances exchanges.

The u-channel proton exchange Lagrangians are given by

$$\mathcal{L}_{\pi NN} = \frac{g_{\pi NN}}{2M_N}\overline{N}\gamma^\mu\gamma^5\partial_\mu\pi\cdot\tau N, \tag{3}$$

$$\mathcal{L}_{KN\Sigma} = \frac{g_{KN\Sigma}}{M_N+M_\Sigma}\overline{\Sigma}\cdot\tau\gamma^\mu\gamma^5 N\partial_\mu\overline{K}, \tag{4}$$

where $g_{\pi NN} = 13.45$ and $g_{KN\Sigma} = 2.69$ from the SU(3) symmetry [16]. We allow an empirical factor [1] between $\frac{1}{\sqrt{2}}$ and $\sqrt{2}$ to multiply to $g_{\pi NN}g_{KN\Sigma}$ for consideration of the SU(3) symmetry breaking effect.

For the s-channel Λ resonance exchanges with different J^P, the effective Lagrangians are as follows:

$$\mathcal{L}_{KN\Lambda(\frac{1}{2}^+)} = \frac{g_{KN\Lambda}}{M_N+M_\Lambda}\partial_\mu\overline{K}\overline{\Lambda}\gamma^\mu\gamma_5 N + \text{H.c.} \tag{5}$$

$$\mathcal{L}_{\Lambda(\frac{1}{2}^+)\pi\Sigma} = \frac{g_{\Lambda\pi\Sigma}}{M_\Lambda+M_\Sigma}\overline{\Sigma}\cdot\partial_\mu\bar{\pi}\gamma^\mu\gamma_5\Lambda + \text{H.c.} \tag{6}$$

$$\mathcal{L}_{KN\Lambda(\frac{1}{2}^-)} = -ig_{KN\Lambda(\frac{1}{2}^-)}\overline{K}\overline{\Lambda}N + \text{H.c.} \tag{7}$$

$$\mathcal{L}_{\Lambda(\frac{1}{2}^-)\pi\Sigma} = -ig_{\Lambda(\frac{1}{2}^-)\pi\Sigma}\overline{\Lambda}\pi\cdot\Sigma + \text{H.c.} \tag{8}$$

$$\mathcal{L}_{KN\Lambda(\frac{3}{2}^+)} = \frac{f_{KN\Lambda(\frac{3}{2}^+)}}{m_K}\partial_\mu\overline{K}\overline{\Lambda}^\mu N + \text{H.c.} \tag{9}$$

$$\mathcal{L}_{\Lambda(\frac{3}{2}^+)\Lambda\pi} = \frac{f_{\Lambda(\frac{3}{2}^+)\pi\Sigma}}{m_\pi}\partial_\mu\overline{\pi}\cdot\overline{\Sigma}\Lambda^\mu + \text{H.c.} \tag{10}$$

$$\mathcal{L}_{KN\Lambda(\frac{3}{2}^-)} = \frac{f_{KN\Lambda(\frac{3}{2}^-)}}{m_K}\partial_\mu\overline{K}\overline{\Lambda}^\mu\gamma_5 N + \text{H.c.} \tag{11}$$

$$\mathcal{L}_{\Lambda(\frac{3}{2}^-)\pi\Sigma} = \frac{f_{\Lambda(\frac{3}{2}^-)\pi\Sigma}}{m_\pi}\partial_\mu\pi\overline{\Lambda}^\mu\gamma_5\Sigma + \text{H.c.} \tag{12}$$

For $\Lambda(1115)\frac{1}{2}^+$, the SU(3) flavor symmetry predicts $g_{KN\Lambda} = -13.98$ and $g_{\Lambda\pi\Sigma} = 9.32$. Considering the SU(3) symmetry breaking effect, we multiply a tunable factor ranged from $\frac{1}{\sqrt{2}}$ to $\sqrt{2}$ to $g_{KN\Lambda}g_{\Lambda\pi\Sigma}$.

For $\Lambda(1405)\frac{1}{2}^-$, we adopt the PDG [5] estimated mass and width for it, i.e., 1405.1 and 50 MeV, respectively. Its coupling to $\pi\Sigma$ is obtained from its decay width to be $g_{\Lambda\pi\Sigma} = 0.9$. Because $\Lambda(1405)$ is below the K^-p threshold, $g_{KN\Lambda(\frac{1}{2}^-)}$ cannot be directly evaluated from the decay approach. Nevertheless, there are many theoretical works on this parameter. Williams *et al.* [17] gave an upper limit for $g_{KN\Lambda(1405)}$ of 3.0 obtained from hadronic scattering. The work of two-pole structure for $\Lambda(1405)$ by Jido *et al.* [3] gives $|g_{\overline{K}N\Lambda}| = 2.1$ for the lower resonance and $|g_{\overline{K}N\Lambda}| = 2.7$ for the upper resonance. By using a separable potential model [18], Xie and Wilkin [19] give $g^2_{KN\Lambda(1405)}/4\pi = 0.27$, i.e., $g_{\Lambda(1405)\overline{K}N} = 1.84$ at the $\overline{K}N$ threshold. In Ref. [16], Xie *et al.* give $g_{\Lambda(1405)\overline{K}N} = 0.77$ and $g_{\Lambda(1405)\overline{K}N} = 1.51$ from two different fitting procedures. In our analysis, we set $g_{\Lambda(1405)\overline{K}N}$ to be a free parameter.

As listed by the PDG [5], $\Lambda(1520)\frac{3}{2}^-$ has very narrow ranges of its mass, width, and branching ratios to $\overline{K}N$ and $\pi\Sigma$; we fix its mass to be 1519.5 MeV and its coupling constants are $f_{KN\Lambda} = 10.5$ and $f_{\Lambda\pi\Sigma} = 2.12$. We use the energy-dependent width of $\Lambda(1520)$, which contains the Blatt-Weisskopf barrier factor [20,21]

$$\Gamma(\sqrt{s}) = \Gamma_0\sum_i\left[c_i\frac{p^3_{B_i}(\sqrt{s})M_{\Lambda^*}\left[E_{B_i}(\sqrt{s})-M_{B_i}\right]B_2^2\left[p_{B_i}(\sqrt{s})\right]}{p^3_{B_i}(M_{\Lambda^*})\sqrt{s}\left[E_{B_i}(M_{\Lambda^*})-M_{B_i}\right]B_2^2\left[p_{B_i}(M_{\Lambda^*})\right]}\right]\Big/\sum_j c_j, \tag{13}$$

where s is the square of the invariant mass of the K^-p system, $\Gamma_0 = 15.6$ MeV, c_i is the branching ratio to the ith final state, $c_{\overline{K}N} = 0.45$, and $c_{\pi\Sigma} = 0.42$ [5]. $p_{B_i}(W)$ and $E_{B_i}(W)$ represent the magnitude of the three-momentum and energy of the baryon in the decayed final system, respectively, i.e., $p^2_{B_i}(W) = \frac{(W^2+M^2_{B_i}-m^2_{M_i})^2}{4W^2} - M^2_{B_i}$ and $E_{B_i}(W) = \sqrt{p^2_{B_i}(W)+M^2_{B_i}}$. $B_2(Q) = \sqrt{\frac{13}{Q^4+3Q^2Q_0^2+9Q_0^4}}$ is the Blatt-Weisskopf barrier factor [20,21] for $l=2$, and Q_0 is a hadron "scale" parameter as a tunable parameter ranging from 0.5 to 1.5 in our analysis.

The $\Lambda(1670)\frac{1}{2}^-$ and $\Lambda(1690)\frac{3}{2}^-$ coupling constants can be deduced from their relevant widths decaying to $\overline{K}N$ and $\Sigma\pi$ as listed in the PDG data [5]. Taking into account their uncertainties, we constrain $g_{\Lambda(1670)\pi\Sigma}g_{KN\Lambda(1670)}$ to be in the range of 0.04–0.2 and $f_{KN\Lambda}f_{\Lambda\pi\Sigma}$ to be in the range of 2.85–7.62 in our fitting. Their masses and widths are also tunable parameters. We give an overview of the fixed value or tuned range of parameters in Table I.

At each vertex, an off-shell form factor is used. For the t-channel K^* meson exchange, we use the form factor

$$F_{K^*}(p^2_{K^*}) = \left(\frac{\Lambda^2-m^2_{K^*}}{\Lambda^2-p^2_{K^*}}\right)^2, \tag{14}$$

where m_{K^*}, p_{K^*}, and Λ are the mass, the four-momentum, and the cutoff parameter for the exchanged K^*.

For the u-channel and s-channel baryon exchanges, the off-shell form factor is in the form

$$F_B(q^2,M) = \frac{\Lambda^4}{\Lambda^4+(q^2-M^2)^2}, \tag{15}$$

TABLE I. Values of fixed parameters and tuned range for fitted parameters.

$g_{K^*K\pi}$	$m_{\Lambda(1115)}$ (MeV)	$m_{\Lambda(1405)}$ (MeV)	$\Gamma_{\Lambda(1405)}$ (MeV)	$m_{\Lambda(1520)}$ (MeV)	$f_{KN\Lambda(1520)}f_{\Lambda(1520)\pi\Sigma}$	Q_0
-3.23	1115.683	1405.1	50	1519.5	22.26	[0.5,1.5]
	$g_{K^*N\Sigma}$	$\kappa_{K^*N\Sigma}$	$g_{\pi NN}g_{KN\Sigma}$	$g_{KN\Lambda(1115)}g_{\Lambda(1115)\pi\Sigma}$	$g_{KN\Lambda(1405)}g_{\Lambda(1405)\pi\Sigma}$	
	$[-3.52,-2.46]$	$[-1.14,-0.47]$	[25.6,51.2]	$[-184.26,-92.13]$	Free	
	$m_{\Lambda(1670)}$ (MeV)	$\Gamma_{\Lambda(1670)}$ (MeV)	$g_{KN\Lambda(1670)}g_{\Lambda(1670)\pi\Sigma}$	$m_{\Lambda(1690)}$ (MeV)	$\Gamma_{\Lambda(1690)}$ (MeV)	$g_{KN\Lambda(1690)}g_{\Lambda(1690)\pi\Sigma}$
	[1600, 1700]	[0, 250]	[0.04,0.2]	[1650, 1750]	[0, 250]	[2.85,7.62]

where M, q, and Λ stand for the mass, the four-momentum, and the cutoff factor of the exchanged baryon. The cutoff parameter is constrained between 0.8 and 1.5 for all channels.

The propagator for the vector meson K^* exchange is

$$G_{K^*}(p_{K^*}) = \frac{-g^{\mu\nu} + p^{\mu}_{K^*}p^{\nu}_{K^*}/m^2_{K^*}}{p^2_{K^*} - m^2_{K^*}}. \tag{16}$$

For the u-channel proton exchange, the propagator is

$$G_B(q) = \frac{\not{q} + m}{q^2 - m^2}. \tag{17}$$

For the s-channel $\Lambda(1115)$ exchange, the expression of the propagator is

$$G_B(q) = \frac{\not{q} + \sqrt{s}}{q^2 - m^2}. \tag{18}$$

For other Λ unstable resonances, the propagators [22] are in the Breit-Weigner forms

$$G_R^{\frac{1}{2}}(q) = \frac{\not{q} + \sqrt{s}}{q^2 - M^2 + iM\Gamma}, \tag{19}$$

$$G_R^{\frac{3}{2}}(q) = \frac{\not{q} + \sqrt{s}}{q^2 - M^2 + iM\Gamma} \times \left(-g^{\mu\nu} + \frac{\gamma^{\mu}\gamma^{\nu}}{3} + \frac{\gamma^{\mu}q^{\nu} - \gamma^{\nu}q^{\mu}}{3\sqrt{s}} + \frac{2q^{\mu}q^{\nu}}{3s}\right), \tag{20}$$

where Γ is the total width of the resonance and s is the square of the invariant mass of the K^-p system.

The differential cross section for $K^-p \to \pi^0\Sigma^0$ in the center-of-mass frame is

$$\frac{d\sigma}{d\Omega} = \frac{1}{64\pi^2 s}\frac{|\mathbf{k}'|}{|\mathbf{k}|}\overline{|\mathcal{M}|}^2, \tag{21}$$

where $d\Omega = 2\pi d\cos\theta$, and θ is the angle between K^- and π^0 in the center-of-mass frame. $\mathbf{k}$ and $\mathbf{k}'$ represent the three-momenta of K^- and π^0 in the c.m. frame, respectively. The amplitude $\mathcal{M}$ and its averged square can be expressed as

$$\mathcal{M}_{\lambda,\lambda'} = u^{\lambda'}_{\Sigma^0}(p')\mathcal{A}u^{\lambda}_{p}(p) = u^{\lambda'}_{\Sigma^0}(p')\sum_i \mathcal{A}_i u^{\lambda}_{p}(p), \tag{22}$$

$$\overline{|\mathcal{M}|}^2 = \frac{1}{2}\sum_{\lambda,\lambda'}\mathcal{M}_{\lambda,\lambda'}\mathcal{M}^{\dagger}_{\lambda,\lambda'} = \frac{1}{2}\mathrm{Tr}[(\not{p}' + M_{\Sigma^0})\mathcal{A}(\not{p} + M_p)\gamma^0\mathcal{A}^{\dagger}\gamma^0], \tag{23}$$

where p and p' represent the four-momenta of protons and Σ^0 separately, λ and λ' stand for the spin index of protons and Σ^0, respectively. $\mathcal{A}$ is the total amplitude despite the spin functions and $\mathcal{A}_i$ denotes the ith channel partial contribution.

The Σ^0 polarization is in the form [23]

$$P_{\Sigma^0} = 2\mathrm{Im}\left(\mathcal{M}_{\frac{1}{2}\frac{1}{2}}\mathcal{M}^*_{-\frac{1}{2}\frac{1}{2}}\right)\Big/\overline{|\mathcal{M}|}^2. \tag{24}$$

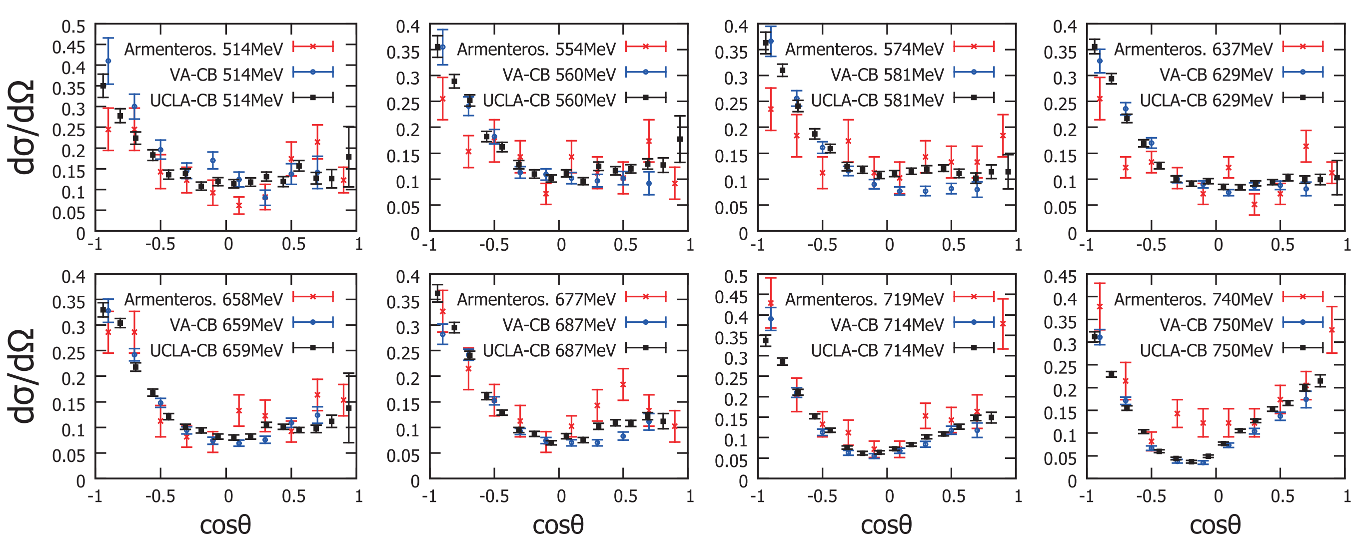

FIG. 2. (Color online) The differential cross sections from Ref. [12], the VA group [10], and the UCLA group [11] of the CB Collaboration at similar beam momenta.

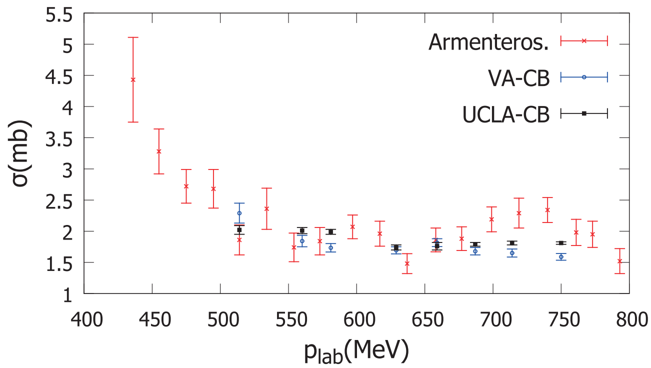

FIG. 3. (Color online) The total cross sections from Ref. [12], the VA group [10], and the UCLA group [11].

III. RESULTS AND DISCUSSIONS

The analyzed experimental data are from Armenteros *et al.* [12], the VA group [10], and the UCLA group [11] of the CB Collaboration. The differential cross-section data of these three references are shown in Fig. 2. We can see that the differential cross sections from the VA group and the UCLA group of the CB Collaboration are compatible with each other, while some data points from Ref. [12] diverge from those of the two CB groups, but with large error bars. Figure 3 shows the total cross-section data of the three references. The total cross sections of the VA group and the UCLA group of the CB Collaboration can be smoothly extended from the four lower-momentum data of Ref. [12]. So we will use the four low-momentum differential cross-section data together with those from the VA group and the UCLA group of the CB Collaboration [10,11].

Considering the distinct polarization results of the VA group and the UCLA group, we first only fit the differential cross sections given consistently by three experimental groups. Then we separately deal with the differential cross sections with either the polarization data of the VA group or the polarization data of the UCLA group.

Our fitting procedure is as follows. First we include the t-channel K^*, the u-channel proton, and the s-channel well-established $\Lambda(1115)$ and its resonances $\Lambda(1405)\frac{1}{2}^-$, $\Lambda(1520)\frac{3}{2}^-$, $\Lambda(1670)\frac{1}{2}^-$, and $\Lambda(1690)\frac{3}{2}^-$ contributions, which contain 19 tunable parameters, and give the results. Second we discuss the results by including an additional Λ resonance with $J^P = \frac{1}{2}^+$, $\frac{1}{2}^-$, $\frac{3}{2}^+$ or $\frac{3}{2}^-$ to the s channel. Then we try to add an additional two, three, and four Λ resonances to see the improvement of the description of the experimental data. Including an additional resonance increases the tunable parameters by 4, i.e., the cutoff parameter, the mass, the width, and the product of coupling constants to $\overline{K}N$ and $\pi\Sigma$ of the resonance.

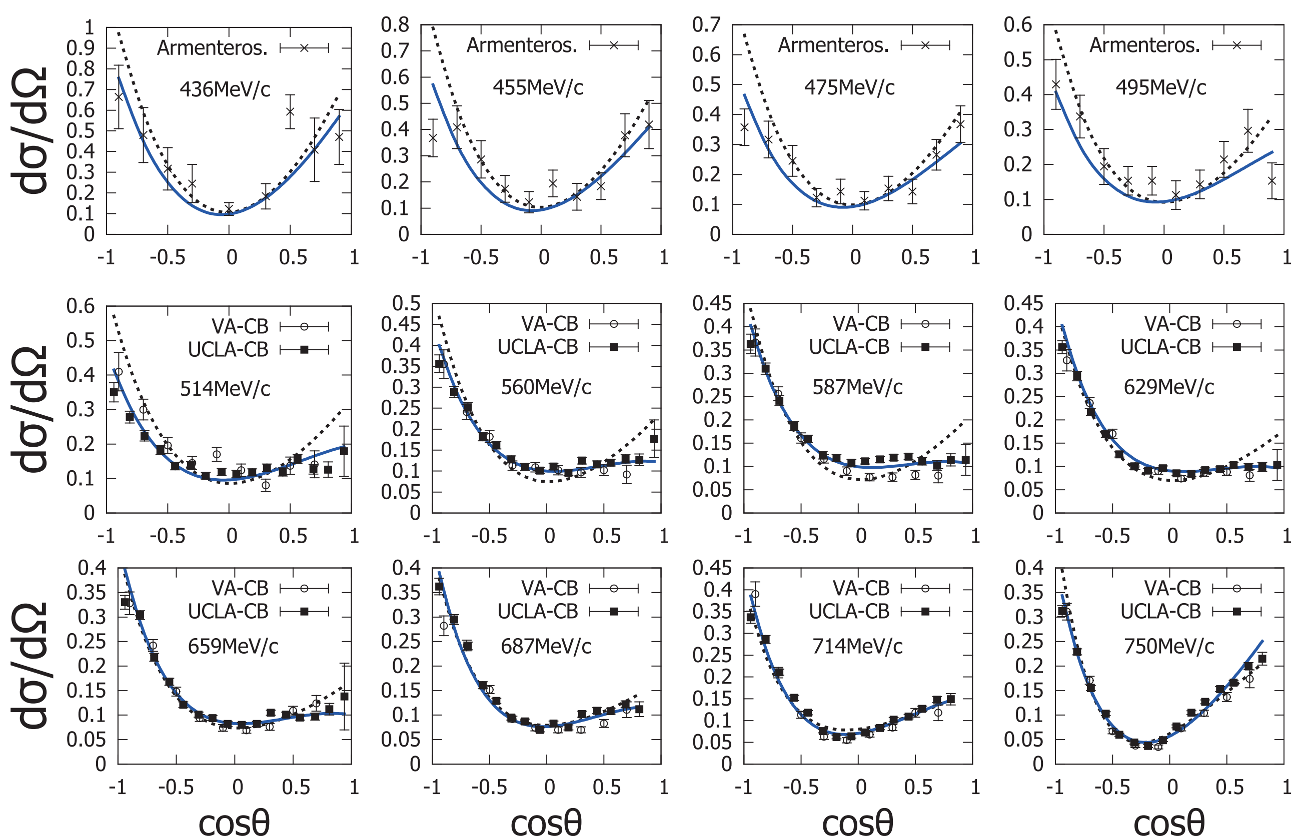

FIG. 4. (Color online) Fit compared with the differential cross-section data from Refs. [10–12]. The dashed lines show results with the inclusion of only five four-star Λ resonances in the s channel; the blue solid lines represent the results of including an additional $\Lambda(\frac{1}{2}^+)$ resonance.

TABLE II. Fitted parameters of $\Lambda(1670)\frac{1}{2}^-$, $\Lambda(1690)\frac{3}{2}^-$ and the additional $\Lambda(\frac{1}{2}^+)$ for the lowest χ^2 result when adding one additional resonance.

	Mass (MeV) (PDG estimate)	$\Gamma_{\rm tot}$ (MeV) (PDG estimate)	$\sqrt{\Gamma_{\pi\Sigma}\Gamma_{\overline{K}N}}/\,\Gamma_{\rm tot}$ (PDG range)
$\Lambda(1670)\frac{1}{2}^-$	1701.8 ± 3.5 (1660, 1680)	127.9 ± 1 (25, 50)	− 0.38 ± 0.043 (−0.38, −0.23)
$\Lambda(1690)\frac{3}{2}^-$	1683.8 ± 1.5 (1685, 1695)	42.4 ± 4.8 (50, 70)	− 0.228 ± 0.037 (−0.34, −0.25)
$\Lambda(1600)\frac{1}{2}^+$	1581.7 ± 32 (1560, 1700)	142.5 ± 4.5 (50, 250)	− 0.365 ± 0.01 (−0.33, 0.28)

TABLE III. Fitted coupling constants for t-channel, u-channel, and s-channel $\Lambda(1115)$ and $\Lambda(1405)\frac{1}{2}^-$.

$g_{K^*N\Sigma}$ (Model)	$\kappa_{K^*N\Sigma}$ (Model)	$g_{\pi NN}g_{KN\Sigma}$ [SU(3)]	$g_{KN\Lambda}g_{\Lambda\pi\Sigma}$ [SU(3)]	$g_{KN\Lambda^*}g_{\Lambda^*\pi\Sigma}$
−3.52 ± 0.69 (−3.52, −2.46)	−1.14 ± 0.06 (−1.14, −0.47)	33.76 ± 1.73 (36.18)	−92.13 ± 4.7 (−130.29)	2.97 ± 0.15

TABLE IV. Fitted parameters when additionally adding a $\frac{1}{2}^+$ resonance, a $\frac{3}{2}^-$ resonance, and a $\frac{3}{2}^+$ resonance for the result with $\chi^2/N = 1.771$.

	Mass (MeV) (PDG estimate)	$\Gamma_{\rm tot}$ (MeV) (PDG estimate)	$\sqrt{\Gamma_{\pi\Sigma}\Gamma_{\overline{K}N}}/\,\Gamma_{\rm tot}$ (PDG range)
$\Lambda(1670)\frac{1}{2}^-$	1662.6 ± 0.5 (1660, 1680)	50 ± 18.3 (25, 50)	−0.21 ± 0.004 (−0.38, −0.23)
$\Lambda(1690)\frac{3}{2}^-$	1695 ± 28.8 (1685, 1695)	60.3 ± 9.1 (50, 70)	−0.051 ± 0.015 (−0.34, −0.25)
$\Lambda(1600)\frac{1}{2}^+$	1574.7 ± 0.5 (1560, 1700)	81.9 ± 1.1 (50, 250)	−0.265 ± 0.002 (−0.33, 0.28)
Additional $\frac{3}{2}^-$	1513.6 ± 0.8	230 ± 2.2	−0.064 ± 0.0003
Additional $\frac{3}{2}^+$	1682.3 ± 0.8	132 ± 0.9	0.287 ± 0.002

TABLE V. Fitted parameters with $\chi^2/N = 1.775$ when dropping $\Lambda(1690)\frac{3}{2}^-$.

	Mass (MeV) (PDG estimate)	$\Gamma_{\rm tot}$ (MeV) (PDG estimate)	$\sqrt{\Gamma_{\pi\Sigma}\Gamma_{\overline{K}N}}/\,\Gamma_{\rm tot}$ (PDG range)	
$\Lambda(1670)\frac{1}{2}^-$	1660.9 ± 0.4 (1660, 1680)	48.3 ± 0.8 (25, 50)	−0.22 ± 0.003 (−0.38, −0.23)	
$\Lambda(1600)\frac{1}{2}^+$	1576.3 ± 0.5 (1560, 1700)	80.7 ± 1.1 (50, 250)	−0.273 ± 0.002 (−0.33, 0.28)	
Additional $\frac{3}{2}^-$	1511.2 ± 1	256 ± 2.9	−0.054 ± 0.003	
Additional $\frac{3}{2}^+$	1679.8 ± 0.7	115.3 ± 0.8	0.295 ± 0.002	
$g_{K^*N\Sigma}$ (Model)	$\kappa_{K^*N\Sigma}$ (Model)	$g_{\pi NN}g_{KN\Sigma}$ [SU(3)]	$g_{KN\Lambda}g_{\Lambda\pi\Sigma}$ [SU(3)]	$g_{KN\Lambda^*}g_{\Lambda^*\pi\Sigma}$
−2.46 ± 1.06 (−3.52, −2.46)	−0.52 ± 0.37 (−1.14, −0.47)	51.2 ± 24.1 (36.18)	−92.13 ± 59.6 (−130.29)	2.49 ± 0.02

TABLE VI. Fitted resonance parameters with $\chi^2/N = 2.17$ when replacing the new $3/2^+$ resonance by $\Lambda(1890)\frac{3}{2}^+$.

	Mass (MeV) (PDG estimate)	$\Gamma_{\rm tot}$(MeV)(PDG estimate)	$\sqrt{\Gamma_{\pi\Sigma}\Gamma_{\overline{K}N}}/\,\Gamma_{\rm tot}$ (PDG range)
$\Lambda(1670)\frac{1}{2}^-$	1670.9 ± 0.5 (1660, 1680)	50 ± 1.2 (25, 50)	−0.19 ± 0.006 (−0.38, −0.23)
$\Lambda(1690)\frac{3}{2}^-$	1695 ± 1.6 (1685, 1695)	70 ± 13.1 (50, 70)	−0.165 ± 0.005 (−0.34, −0.25)
$\Lambda(1600)\frac{1}{2}^+$	1563.2 ± 0.2 (1560, 1700)	159 ± 0.4 (50, 250)	−0.337 ± 0.001 (−0.33, 0.28)
$\Lambda(1890)\frac{3}{2}^+$	1850 ± 0.5 (1850, 1910)	200 ± 0.1 (60, 200)	0.99 ± 0.002
Additional $\frac{3}{2}^-$	1558.3 ± 0.9	130.6 ± 2.8	−0.05 ± 0.0002

TABLE VII. Fitted parameters for the best fit of $\chi^2/N = 1.71$ when adding four additional resonances.

J^P	Mass (MeV)	$\Gamma_{\rm tot}$ (MeV)	$\sqrt{\Gamma_{\pi\Sigma}\Gamma_{\bar{K}N}}/\Gamma_{\rm tot}$
$\frac{1}{2}^+$	1580.3 ± 1.3	67.8 ± 2.6	-0.24 ± 0.002
$\frac{1}{2}^+$	1544.8 ± 1	36.3 ± 2.5	-0.21 ± 0.006
$\frac{3}{2}^-$	1505.2 ± 1.4	274.4 ± 2.2	-0.049 ± 0.0002
$\frac{3}{2}^+$	1680.7 ± 1.1	144.9 ± 2.3	0.281 ± 0.002

TABLE VIII. Fitted parameters for $\chi^2/N = 1.70$ when adding four additional resonances including one $\frac{5}{2}^-$ resonance.

J^P	Mass (MeV)	$\Gamma_{\rm tot}$ (MeV)	$\sqrt{\Gamma_{\pi\Sigma}\Gamma_{\bar{K}N}}/\Gamma_{\rm tot}$
$\frac{1}{2}^+$	1578.3 ± 0.85	73.7 ± 1.6	-0.252 ± 0.003
$\frac{3}{2}^+$	1681.3 ± 1.1	112.8 ± 1.1	-0.292 ± 0.003
$\frac{3}{2}^-$	1500 ± 5.4	280.4 ± 3.7	-0.043 ± 0.001
$\frac{5}{2}^-$	1578 ± 4.7	44.3 ± 9	0.13 ± 0.02

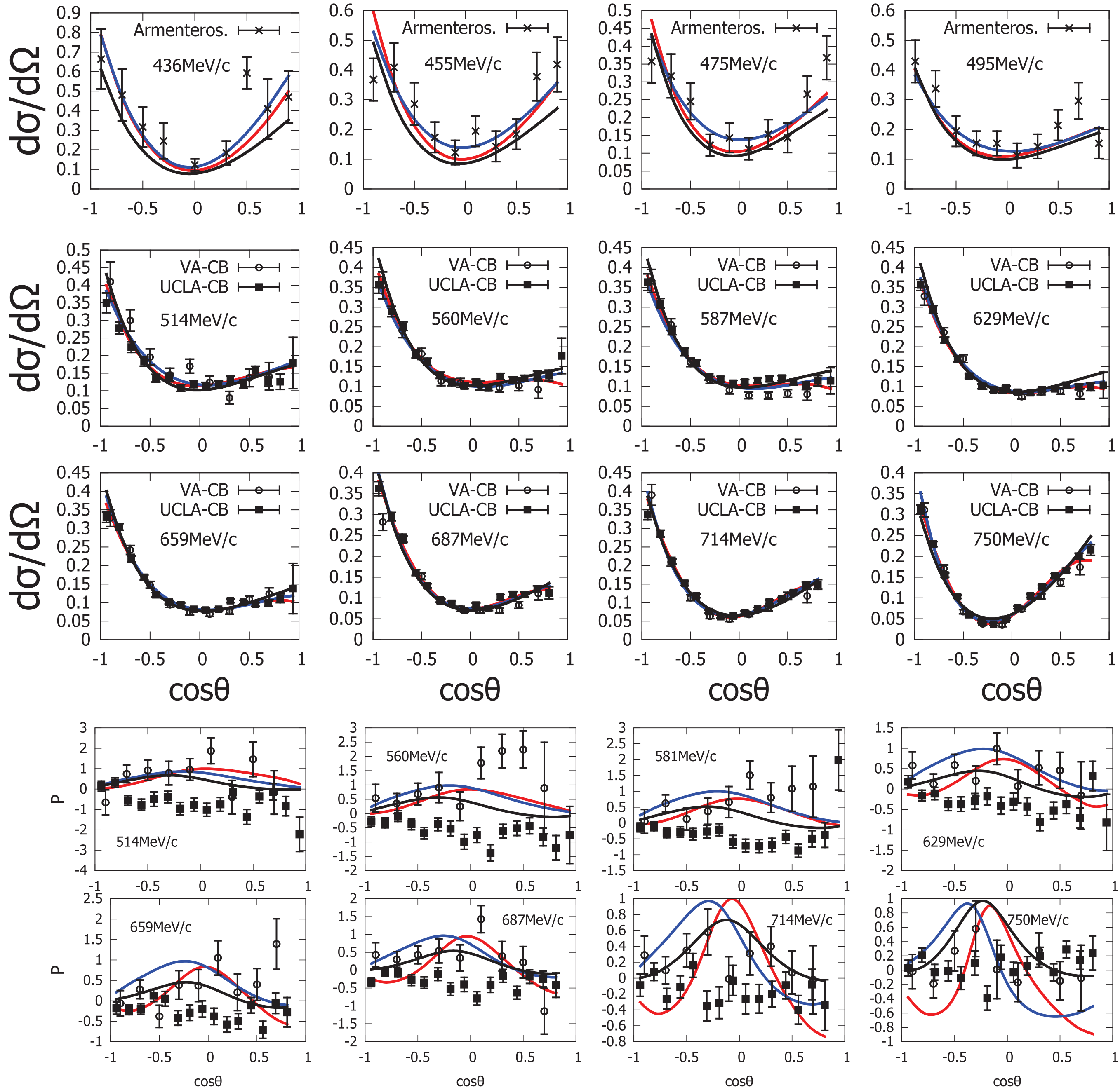

FIG. 5. (Color online) The most favored fit (red solid lines) to the differential cross-section data from Refs. [10–12], and the corresponding prediction to the polarizations compared with the data of Refs. [10,11]. As a comparison, fits by dropping the $\frac{3}{2}^+$ resonance or by replacing it with $\Lambda(1690)\frac{3}{2}^-$ are shown with blue dashed and black dot-dashed lines, respectively.

A. Results of fitting only the differential cross-section data from Refs. [10–12]

When only fitting the 236 differential cross-section data points of Refs. [10–12], the fit without adding additional Λ resonances in the s channel has χ^2 per data point equaling 6.21. The fit compared with the experimental data is shown in Fig. 4 by the dashed lines.

When adding one additional resonance, the best fit is to add a $J^P = \frac{1}{2}^+$ resonance, with mass around 1582 MeV and width about 142 MeV, leading to $\chi^2/N = 2.77$. The fitting results are shown in Fig. 4. The fitted parameters and uncertainties for $\Lambda(1670)\frac{1}{2}^-$, $\Lambda(1690)\frac{3}{2}^-$, and the added $\Lambda(\frac{1}{2}^+)$ of this solution together with the lower and upper limits of the PDG estimates or ranges are shown in Table II. Here and later, the uncertainties include only the statistical error bars given automatically by the standard CERNLIB fitting code MINUIT. The fitted couplings for t-channel K^*, u-channel proton, and s-channel Λ(1115) and Λ(1405) are shown in Table III.

Instead of the $\frac{1}{2}^+$ resonance, when adding a $\frac{3}{2}^-$ resonance, the χ^2/N is 2.91, with the resonance's mass being about 1526 MeV and its width being near 43 MeV. The other results for adding one additional resonance are $\chi^2/N = 4.36$ for adding one $J^P = \frac{3}{2}^+$ resonance and $\chi^2/N = 3.75$ for adding one $J^P = \frac{1}{2}^-$ resonance.

When adding two additional resonances, the lowest χ^2/N equaling 2.29 is given by adding a $\frac{1}{2}^+$ resonance and a $\frac{3}{2}^-$ resonance. The parameters for the $\frac{1}{2}^+$resonance are mass around 1604 ± 3.3 MeV, width about 248 ± 3.4 MeV, and coupling $\sqrt{\Gamma_{\pi\Sigma}\Gamma_{\overline{K}N}}/\Gamma_{\rm tot} = -0.31 \pm 0.02$. The $\frac{3}{2}^-$ resonance's mass, width, and branching ratio are 1535 ± 3.3 MeV, 29 ± 8 MeV, and $\sqrt{\Gamma_{\pi\Sigma}\Gamma_{\overline{K}N}}/\Gamma_{\rm tot} = -0.11 \pm 0.02$, respectively.

The second lowest result for adding two additional resonances is to add a $\frac{3}{2}^+$ resonance in additional to the $\frac{1}{2}^+$ resonance, leading to a χ^2/N of 2.31, which is very close to the result obtained by adding a $\frac{3}{2}^-$ resonance in addition to the $\frac{1}{2}^+$ resonance. The fitted parameters for the $\frac{3}{2}^+$ resonance are mass of about 1680 ± 0.8 MeV, width near 39 ± 1.3 MeV, and branching ratio $\sqrt{\Gamma_{\pi\Sigma}\Gamma_{\overline{K}N}}/\Gamma_{\rm tot} = 0.11 \pm 0.003$. Meanwhile, the mass, width, and couplings of $\frac{1}{2}^+$ are shifted to 1574 ± 0.4 MeV, 132 ± 0.7 MeV, and $\sqrt{\Gamma_{\pi\Sigma}\Gamma_{\overline{K}N}}/\Gamma_{\rm tot} = -0.34 \pm 0.001$.

The best result for adding three resonances is to add one $\frac{1}{2}^+$ resonance, one $\frac{3}{2}^-$ resonance, and one $\frac{3}{2}^+$ resonance, with χ^2/N equaling 1.771. The adjusted parameters for the established Λ(1670) and Λ(1690) together with the additional three resonances are shown in Table IV.

Because adding these additional resonances significantly reduces the contribution of $\Lambda(1690)\frac{3}{2}^-$, we examine whether it is really needed by the data. It is found that dropping $\Lambda(1690)\frac{3}{2}^-$ only increases the χ^2/N by 0.004 to be 1.775, while dropping any other resonance will increase χ^2/N by more than 0.5. This indicates that $\Lambda(1690)\frac{3}{2}^-$ is indeed not needed by the data. The fitted parameters are shown in Table V.

Further, when we replace the $\frac{3}{2}^+$ resonance by the well established $\Lambda(1890)\frac{3}{2}^+$ with mass from 1850 to 1910 MeV and width from 60 to 200 MeV [5], χ^2/N is 2.17. The fitted parameters of the five resonances are shown in Table VI. This demonstrates that the new $\frac{3}{2}^+$ resonance around 1680 MeV cannot be replaced by the well-established $\Lambda(1890)\frac{3}{2}^+$.

The best fit by adding four additional resonances has $\chi^2/N = 1.71$, by adding two $\frac{1}{2}^+$ resonances, one $\frac{3}{2}^-$ resonance, and one $\frac{3}{2}^+$ resonance. Their fitted parameters are shown in Table VII. The two $\frac{1}{2}^+$ resonances strongly overlap and can be regarded as some modification to the shape of one resonance. Moreover, the fit improves χ^2/N only by 0.065 with four additional parameters. This suggests that there is no evidence for any more resonances from the data.

From our above investigation, we regard the fit given in Table V as our most favored fit to the CB data on the differential cross sections. In this most favored fit, the PDG four-star resonance $\Lambda(1670)\frac{1}{2}^-$ and three-star resonance $\Lambda(1600)\frac{1}{2}^+$ are definitely needed with fitted parameters compatible with PDG values; the PDG four-star resonance $\Lambda(1690)\frac{3}{2}^-$ is dropped, replaced by a new $\Lambda(1680)\frac{3}{2}^+$ resonance; an additional broad $3/2^-$ contribution couples to this channel weakly and may be regarded as a modification to the tail of $\Lambda(1520)\frac{3}{2}^-$. The fitted results of this most favored solution are shown in Fig. 5, together with the predicted polarizations of this solution compared with two sets of CB polarization data from Refs. [10,11]. The predicted polarizations are more inclined to the data from the VA group [10]. As a comparison, fits by dropping the $\frac{3}{2}^+$ resonance with $\chi^2/N = 3.23$ or replacing it by $\Lambda(1690)\frac{3}{2}^-$ with $\chi^2/N = 2.29$ are also shown in Fig. 5 by blue dashed and black dot-dashed lines, respectively.

For higher spin resonances, we try adding one $\frac{5}{2}^-$ resonance to our most favored fit. When constraining the parameters

TABLE IX. Refitted parameters for our most favored solution with $\chi^2/N = 1.79$ when including polarization data from the VA group of the CB Collaboration [10].

	Mass (MeV) (PDG estimate)	$\Gamma_{\rm tot}$ (MeV) (PDG estimate)	$\sqrt{\Gamma_{\pi\Sigma}\Gamma_{\overline{K}N}}/\Gamma_{\rm tot}$ (PDG range)	
$\Lambda(1670)\frac{1}{2}^-$	1662.5 ± 0.3 (1660, 1680)	50 ± 0.7 (25, 50)	-0.29 ± 0.003 (-0.38, -0.23)	
$\Lambda(1600)\frac{1}{2}^+$	1575.2 ± 0.6 (1560, 1700)	94.8 ± 1 (50, 250)	-0.293 ± 0.002 (-0.33, 0.28)	
Additional $\frac{3}{2}^-$	1506.9 ± 1.4	334.4 ± 3.4	-0.04 ± 0.002	
Additional $\frac{3}{2}^+$	1687.7 ± 1	112.7 ± 0.8	0.297 ± 0.002	
$g_{K^*N\Sigma}$ (Model)	$\kappa_{K^*N\Sigma}$ (Model)	$g_{\pi NN}g_{KN\Sigma}$ [SU(3)]	$g_{KN\Lambda}g_{\Lambda\pi\Sigma}$ [SU(3)]	$g_{KN\Lambda^*}g_{\Lambda^*\pi\Sigma}$
-3.52 ± 0.75 (-3.52, -2.46)	-1.14 ± 0.11 (-1.14, -0.47)	28.8 ± 1.3 (36.18)	-92.13 ± 9.4 (-130.29)	2.16 ± 0.03

of the $\frac{5}{2}^-$ resonance in the $\Lambda(1830)\frac{5}{2}^-$ range of the PDG estimate [5], i.e., mass between 1810 and 1830 MeV, width from 60 to 110 MeV, and coupling $\sqrt{\Gamma_{\pi\Sigma}\Gamma_{\overline{K}N}}/\Gamma_{\rm tot}$ from -0.17 to -0.13, χ^2/N improves by negligible 0.01 to be 1.765. If all parameters are allowed to be free, the resulting χ^2/N is 1.70. The improvement of χ^2/N is still not significant. Adjusted parameters for resonances are shown in Table VIII, where the influence on other resonances is small.

Because the two sets of CB polarization data from Refs. [10,11] are not consistent with each other, we examine in the following two subsections how each set of the polarization data influences our solution separately.

B. Fitting the differential cross sections of Refs. [10–12] and polarization data from the VA group of the CB Collaboration [10]

Based on our most favored solution in the last subsection, we refit the data by including the polarization data from the VA group of the CB Collaboration [10]. The χ^2 per data point is 1.79 for the 308 experimental data points. The refitted

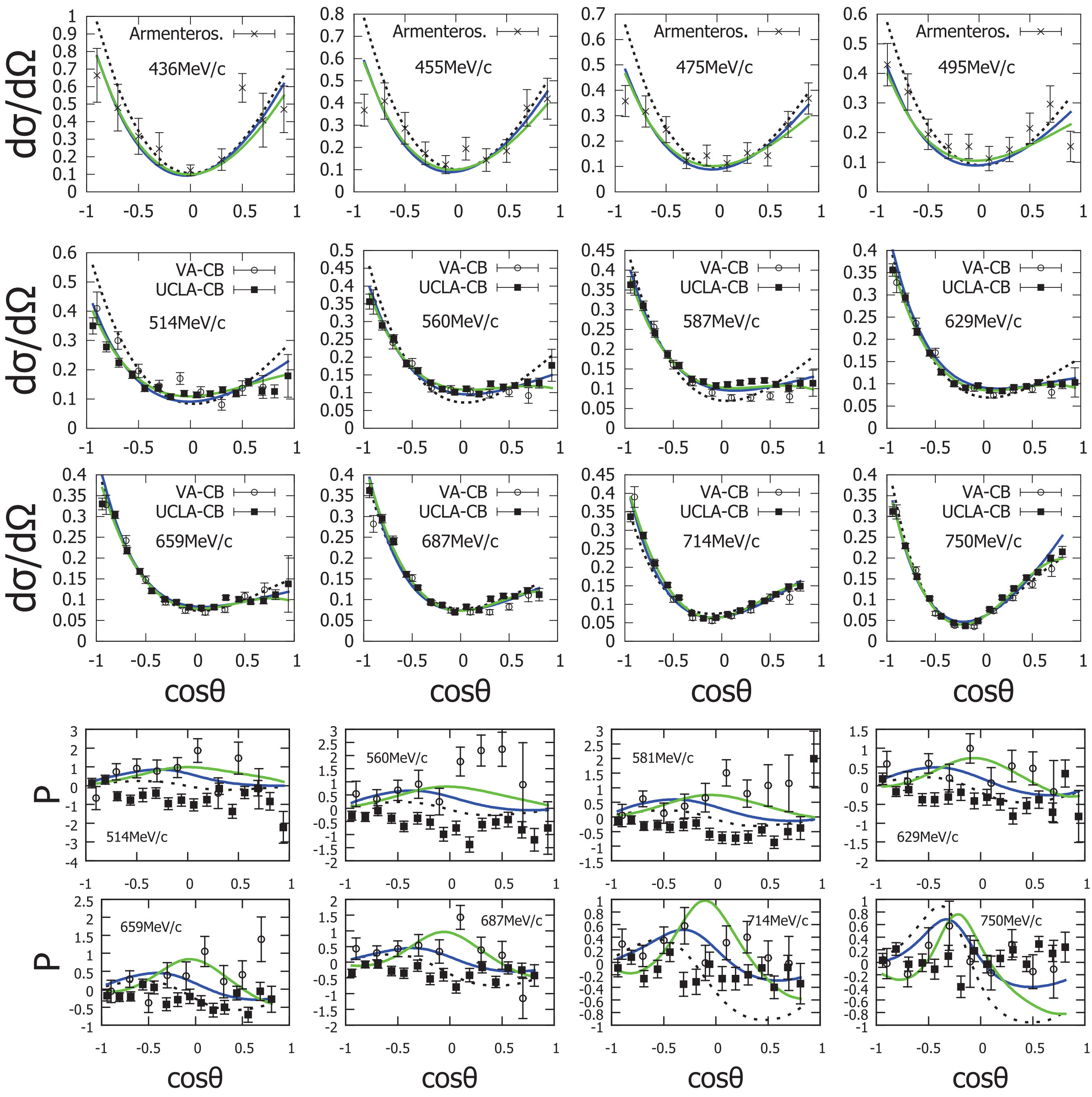

FIG. 6. (Color online) Fits compared with the differential cross-section data of Refs. [10–12] and the polarization data of Refs. [10,11]. The dashed lines represent the results with four-star resonances only, the blue solid lines stand for the results when adding the three-star $\Lambda(1600)\frac{1}{2}^+$ resonance, and the green solid lines show the results of the most favored solution.

parameters of $\Lambda(1670)\frac{1}{2}^-$ and the three additional resonances as well as the couplings for t-channel K^*, u-channel proton, and s-channel $\Lambda(1115)$ and $\Lambda(1405)$ are shown in Table IX, The fits compared with data are shown in Fig. 6.

The refitted parameters are quite similar to those without including the polarization data. Once again, the four-star resonance $\Lambda(1690)\frac{3}{2}^-$ is not needed. Adding it into our present solution only improves χ^2/N by 0.002. Improvement by adding any new resonance with other quantum numbers is also insignificant. Dropping either the $3/2^-$ resonance or the $3/2^+$ resonance in Table IX will increase the χ^2/N by more than 0.42.

C. Fitting the differential cross sections of Refs. [10–12] and polarization data from the UCLA group of the CB Collaboration [11]

If we refit the data using the polarization data from the UCLA group [11] instead of the polarization data from the VA group of the CB Collaboration [10] for our most favored

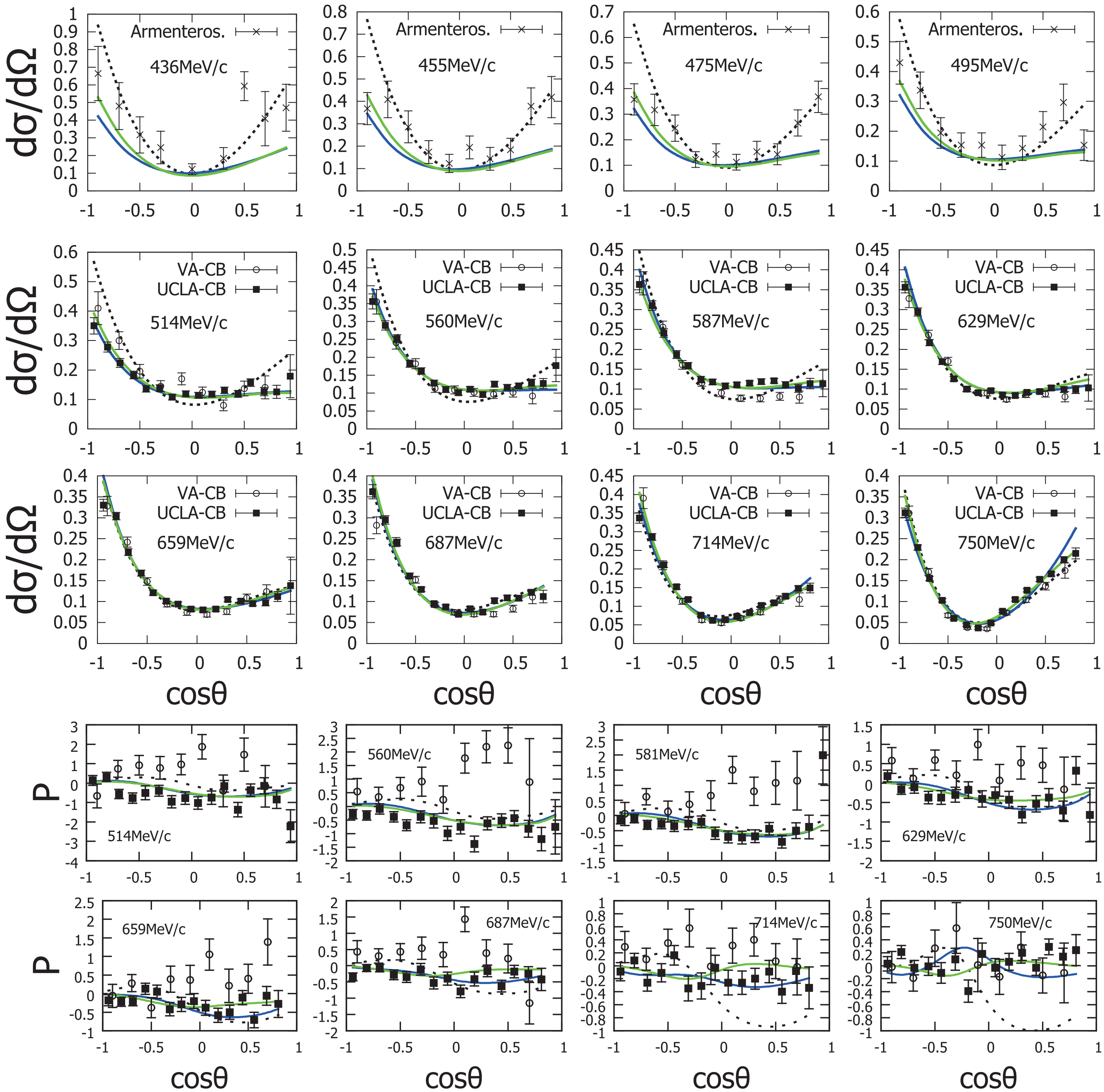

FIG. 7. (Color online) Fits compared with the differential cross-section data of Refs. [10–12] and the polarization data of Refs. [10,11]. The dashed lines represent the results with four-star resonances only, the blue solid lines stand for the results when adding the three-star $\Lambda(1600)\frac{1}{2}^+$ resonance, and the green solid lines show the results of our most favored solution.

TABLE X. Refitted parameters for our most favored solution with $\chi^2/N = 2.45$ when including polarization data from the UCLA group of the CB Collaboration [11].

	Mass (MeV) (PDG estimate)	Γ_{tot} (MeV) (PDG estimate)	$\sqrt{\Gamma_{\pi\Sigma}\Gamma_{\overline{K}N}}/\Gamma_{\text{tot}}$ (PDG range)	
$\Lambda(1670)\frac{1}{2}^-$	1674.2 ± 0.6 (1660, 1680)	30 ± 1 (25, 50)	-0.12 ± 0.004 (-0.38, -0.23)	
$\Lambda(1600)\frac{1}{2}^+$	1557.1 ± 0.4 (1560, 1700)	169.7 ± 0.7 (50, 250)	-0.36 ± 0.001 (-0.33, 0.28)	
Additional $\frac{3}{2}^-$	1585.4 ± 2.4	58.4 ± 4.5	-0.035 ± 0.001	
Additional $\frac{3}{2}^+$	1665.6 ± 1.1	136.5 ± 3	-0.136 ± 0.003	
$g_{K^*N\Sigma}$ (Model)	$\kappa_{K^*N\Sigma}$ (Model)	$g_{\pi NN}g_{KN\Sigma}$ [SU(3)]	$g_{KN\Lambda}g_{\Lambda\pi\Sigma}$ [SU(3)]	$g_{KN\Lambda^*}g_{\Lambda^*\pi\Sigma}$
-3.47 ± 0.8 (-3.52, -2.46)	-0.92 ± 0.5 (-1.14, -0.47)	39.13 ± 0.5 (36.18)	-92.13 ± 4.6 (-130.29)	0.5 ± 0.06

solution, the χ^2/N is 2.45 for the 360 experimental data points. The refitted parameters of $\Lambda(1670)\frac{1}{2}^-$ and the three additional resonances as well as the couplings for t-channel K^*, u-channel proton, and s-channel $\Lambda(1115)$ and $\Lambda(1405)$ are shown in Table X. The fits compared with data are shown in Fig. 7.

Compared with using the polarization data of the VA group, the refitted parameters by using the UCLA data have larger differences from those without including the polarization data. Including the four-star resonance $\Lambda(1690)\frac{3}{2}^-$ improves χ^2/N by 0.09, still much less significant than other resonances. Dropping the $3/2^+$ resonance or the $3/2^-$ resonance in Table X will increase the χ^2/N by 0.54 or 0.29, respectively.

IV. SUMMARY

We have analyzed the $K^-p \to \pi^0\Sigma^0$ reaction using an effective Lagrangian approach. By fitting different sets of experimental data from the CB Collaboration, we reach the following conclusions.

The four-star $\Lambda(1670)\frac{1}{2}^-$ and three-star $\Lambda(1600)\frac{1}{2}^+$ resonances listed in the PDG data [5] are definitely needed no matter which set of CB data is used. As shown in Table V for our most favored solution, the fitted parameters for these two resonances are consistent with their PDG values. In addition, there is strong evidence for the existence of a new $\Lambda(\frac{3}{2}^+)$ resonance around 1680 MeV. It improves χ^2 by more than 100 no matter which set of data is used. It makes a large contribution to this reaction, replacing the contribution from the four-star $\Lambda(1690)\frac{3}{2}^-$ resonance included by previous fits to this reaction. Including some broad $3/2^-$ contribution also improves χ^2 significantly. It couples to this channel weakly and may be regarded as a modification to the tail of $\Lambda(1520)\frac{3}{2}^-$.

Replacing the PDG $\Lambda(1690)\frac{3}{2}^-$ resonance with a new $\Lambda(1680)\frac{3}{2}^+$ resonance has important implications for hyperon spectroscopy and its underlying dynamics. While the classical qqq constituent quark model [24] predicts the lowest $\Lambda(\frac{3}{2}^+)$ resonance to be around 1900 MeV, which is consistent with $\Lambda(1890)\frac{3}{2}^+$ listed in the PDG data, the penta-quark dynamics [25] predicts it to be below 1700 MeV, which is in accordance with $\Lambda(1680)\frac{3}{2}^+$ claimed in this work.

A recent analysis [9] of CB data on the $K^-p \to \eta\Lambda$ reaction requires a $\Lambda(\frac{3}{2}^-)$ resonance with a mass of about 1670 MeV and a width of about 1.5 MeV instead of the well-established $\Lambda(1690)\frac{3}{2}^-$ resonance with a width of around 60 MeV. Together with $N^*(1520)\frac{3}{2}^-$, $\Sigma(1542)\frac{3}{2}^-$ suggested in Ref. [2], and either $\Xi(1620)$ or $\Xi(1690)$, the narrow $\Lambda(1670)\frac{3}{2}^-$ fits in a nice $3/2^-$ baryon nonet with a large penta-quark configuration, i.e., $N^*(1520)$ as the $|[ud]\{uq\}\bar{q}\rangle$ state, $\Lambda(1520)$ as the $|[ud]\{sq\}\bar{q}\rangle$ state, $\Lambda(1670)$ as the $|[ud]\{ss\}\bar{s}\rangle$ state, and $\Xi(16xx)$ as the $|[ud]\{ss\}\bar{q}\rangle$ state. Here $\{q_1q_2\}$ means a diquark with configuration of flavor representation **6**, spin 1, and color $\bar{3}$. $\Lambda(1670)$ as the $|[ud]\{ss\}\bar{s}\rangle$ state gives a natural explanation for its dominant $\eta\Lambda$ decay mode with a very narrow width due to its very small phase space and the suppression of D-wave decay [26].

It would be very important to recheck other relevant reactions whether the new claimed $\Lambda(1680)\frac{3}{2}^+$ is also needed there and may replace the PDG's well-established $\Lambda(1690)\frac{3}{2}^-$. Further precise polarization data for $\overline{K}N$ reactions would be very helpful to clarify the ambiguities in the determination of spin-parities of these hyperon resonances.

ACKNOWLEDGMENTS

Helpful discussions with Bo-Chao Liu, Pu-Ze Gao, Jia-Jun Wu, Ju-Jun Xie, Xu Cao, and W. Briscoe are gratefully acknowledged. This work is supported by the National Natural Science Foundation of China under Grants No. 11035006, No. 11121092, and No. 11261130311 (for the Sino-German CRC110 by DFG and NSFC) and the Chinese Academy of Sciences under Project No. KJCX2-EW-N01.

[1] Puze Gao, B. S. Zou, and A. Sibirtsev, Nucl. Phys. A **867**, 41 (2011).

[2] Puze Gao, Jun Shi, and B. S. Zou, Phys. Rev. C **86**, 025201 (2012).

[3] D. Jido *et al.*, Nucl. Phys. A **725**, 181 (2003).

[4] V. K. Magas, E. Oset, and A. Ramos, Phys. Rev. Lett. **95**, 052301 (2005).

[5] K. A. Olive *et al.* (Particle Data Group), Chin. Phys. C **38**, 090001 (2014).

[6] H. Zhang, J. Tulpan, M. Shrestha, and D. M. Manley, Phys. Rev. C **88**, 035204 (2013); **88**, 035205 (2013).
[7] H. Kamano, S. X. Nakamura, T.-S. H. Lee, and T. Sato, Phys. Rev. C **90**, 065204 (2014).
[8] X. H. Zhong and Q. Zhao, Phys. Rev. C **79**, 045202 (2009); **88**, 015208 (2013).
[9] B. C. Liu and J. J. Xie, Phys. Rev. C **85**, 038201 (2012); **86**, 055202 (2012).
[10] R. Manweiler *et al.*, Phys. Rev. C **77**, 015205 (2008).
[11] S. Prakhov *et al.*, Phys. Rev. C **80**, 025204 (2009).
[12] R. Armenteros *et al.*, Nucl. Phys. B **21**, 15 (1970).
[13] A. Mueller-Groeling, K. Holinde, and J. Speth, Nucl. Phys. A **513**, 557 (1990).
[14] V. G. J. Stoks and T. A. Rijken, Phys. Rev. C **59**, 3009 (1999).
[15] Y. Oh, K. Nakayama, and T.-S. H. Lee, Phys. Rep. **423**, 49 (2006).
[16] J. J. Xie, B. C. Liu, and C. S. An, Phys. Rev. C **88**, 015203 (2013).
[17] R. A. Williams, C. R. Ji, and S. R. Cotanch, Phys. Rev. C **43**, 452 (1991).
[18] N. V. Shevchenko, A. Gal, and J. Mareš, Phys. Rev. Lett. **98**, 082301 (2007); N. V. Shevchenko, A. Gal, J. Mareš, and J. Révai, Phys. Rev. C **76**, 044004 (2007).
[19] J. J. Xie and C. Wilkin, Phys. Rev. C **82**, 025210 (2010).
[20] B. S. Zou and D. V. Bugg, Eur. Phys. J. A **16**, 537 (2003).
[21] S. U. Chung, Phys. Rev. D **48**, 1225 (1993).
[22] A. V. Anisovich *et al.*, Phys. At. Nucl. **74**, 418 (2011).
[23] G. Penner and U. Mosel, Phys. Rev. C **66**, 055211 (2002).
[24] S. Capstick and N. Isgur, Phys. Rev. D **34**, 2809 (1986); S. Capstick and W. Roberts, Prog. Part. Nucl. Phys. **45**, S241 (2000).
[25] C. Helminen and D. O. Riska, Nucl. Phys. A **699**, 624 (2002).
[26] B. S. Zou, Nucl. Phys. A **914**, 454 (2013).